JOURNAL OF AIRCRAFT
Vol. 44, No. 6, November–December 2007

Investigation of the Effect of Metallic Fuselage Dents on Compressive Failure Loads

N. C. Lang and Y. W. Kwon*
Naval Postgraduate School, Monterey, California 93943

DOI: 10.2514/1.31207

The effect of dents in metallic aircraft fuselage was examined on the compressive failure load using the finite element method. The study considered a single impact dent on two different fuselage panels at various locations and impact speeds. The material used for the finite element models was aluminum alloy 2024-T3, a typical material used for fuselages of old transport aircraft. The finite element model consisted of impact analysis followed by either linear eigenvalue analysis or postbuckling compression analysis. These analyses were performed on both stiffened and unstiffened aluminum panels. It was found that, depending on a dent status in an aluminum panel, the dent might increase or decrease the compressive failure load of the panel compared with that of the virgin panel without a dent. The compressive failure load of a panel after a low-velocity impact was generally lower than that of the virgin plate. As the impact velocity increased, the failure load of the dented panel increased, exceeding that of its virgin plate. In addition, the existence of a critical impact velocity was noticed, at which the failure load of the dented panel reached maximum and after which it started to decrease.

I. Introduction

WITH today's rapid increase in the number of aging aircraft, the aerospace industry has fought to reduce costs on maintenance and repair. Life extension of aircraft structures has become a major focus of the industry. The two main costly problems that have caught the attention of the scientific community have been the fight against fatigue and corrosion [1]. Many studies have been and are actively being conducted on crack fatigue, multiple site damages, aircraft skin inspection technology, and others [2]. There is very extensive literature on those topics. Some of them are provided in [3–8].

Although a tremendous workload has been spent on dent repairs and removal in large transport aircraft, little research has been conducted on investigating the effect of dents on the strength of aircraft fuselage panels, to the best knowledge of the authors. After an extensive literature search and review, only a few studies have been found to involve impact damages on metallic airplane structure. One in particular performed an experimental (with some computer modeling) study on fuselage dents [9]. The study used a special impact swing hammer to develop various dent sizes on an Al-2024-T3 fuselage panel. Although this paper focused mainly on fatigue investigation, it did present some static loading data for comparison.

The present work examined the effect of dents in metallic aircraft fuselage on the compressive failure load using the finite element method. The study considered a single impact dent on two different fuselage panels at various locations and impact speeds. The material used for the finite element models was aluminum alloy 2024-T3, a typical material used for fuselages of old transport aircraft. The finite element model consisted of impact analysis followed by either linear eigenvalue analysis or postbuckling compression analysis. These analyses were performed on both stiffened and unstiffened aluminum panels. In addition, linear eigenvalue analysis was also conducted for virgin panels before impact damages, as their reference buckling loads.

The next section describes various finite element modeling and analyses used for this study, and the subsequent section presents the results and discussion. Finally, conclusions are provided at the end.

II. Finite Element Modeling and Analysis

Both stiffened and unstiffened panels were considered in this study. The panels were 0.508 by 0.508 m (20 by 20 in.) and 0.1588 cm (0.625 in.) thick. The stiffened panel consisted of a set of hat stiffeners 20.32 cm (8 in.) apart. Each of the joints between a stiffener and the main panel was modeled to be twice as thick as the main panel itself. The height and width of the winged portion of each stiffener were both 1.905 cm (0.75 in.). The mesh size was the same for both stiffened and unstiffened panels. Their geometries and finite element meshes are shown in Figs. 1 and 2, respectively. The material property was defined as elastic–plastic with linear hardening. The properties used in the models are tabulated in Table 1.†

For finite element analysis, ABAQUS [10] was used. First, linear eigenvalue analysis was undertaken for both panels to determine the buckling loads of the virgin panels before impact damage. These buckling loads were used as the reference values to be compared with the compressive failure loads after impact damage. The two opposite edges of each panel were simply supported and the other two opposite edges remained free. The buckling load was applied to the simply supported edges.

Nonlinear dynamic impact analysis was conducted for each virgin panel. The impactor was a 5.08-cm-diam (2-in.-diam) rigid ball with mass of 1 kg. It hit the center of the unstiffened panel. As far as the stiffened panel is concerned, the impactor struck it either in the middle of the two stiffeners or directly at one stiffener site. All panels were fixed along all the edges during the impact. For impact analysis of each panel, various impact velocities were applied from 10 to 70 m/s. Under each impact, all panels underwent elastic–plastic deformations, resulting in dents and residual stresses and strains. During the contact-impact process, friction was neglected. The list of different impact study cases is summarized in Table 2.

After impact analysis of each panel under each different impact condition, the dent geometry and the residual stresses and strains resulting from the impact were imported into the next analysis model. Then, as a postbuckling analysis, a compressive incremental in-plane load was applied to the damaged panel that had two simply supported edges normal to the loading direction and two other free edges. The

Received 6 April 2007; accepted for publication 17 August 2007.

*Department of Mechanical and Astronautical Engineering, 700 Dyer Road. Corresponding Author

†Data available online at http://www.matweb.com [retrieved 27 March 2007].

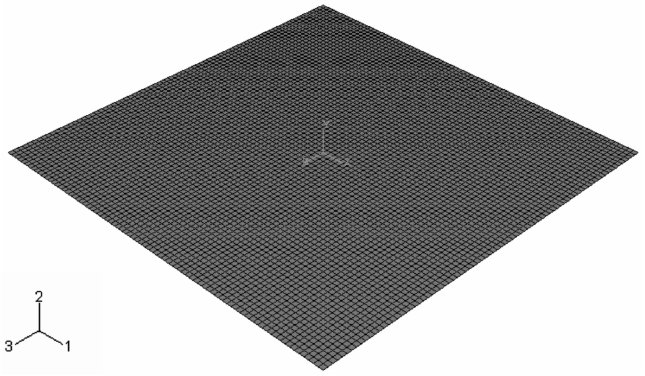

Fig. 1 Finite element mesh of unstiffened panel.

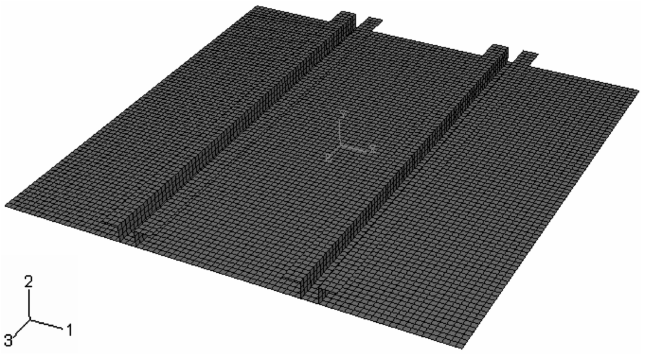

Fig. 2 Finite element mesh for stiffened panel.

load-displacement curve was obtained to determine the compressive failure load after the impact damage. This failure load was compared with the buckling load of the virgin panel.

Instead of the postbuckling analysis, the damaged panels after impact were analyzed for linear eigenvalue analysis to compute the buckling loads of the dented panels. Therefore, the geometries of the impacted panels including dents were imported into the analysis models. However, the residual stresses and strains were not imported. The purpose of this analysis was to find out how critical the residual stresses and strains were in terms of the failure strength of the damaged panels by comparing the buckling loads after impact to the postbuckling compressive failure loads after the same impact.

Table 1 Material property of shell plate Al-2024T3

Young's modulus of elasticity	73.1 GPa
Yield strength	345 MPa
Ultimate strength	483 MPa
Mass density	2780 kg/m^3
Elongation at failure	15%

Table 2 Fuselage panel impact study summary

Panel type	Impactor	Impact location	Impactor speed, m/s
Unstiffened panel	Ball	Center	10
	Ball	Center	30
	Ball	Center	35
	Ball	Center	55
	Ball	Center	60
	Ball	Center	65
	Ball	Center	70
Stiffened panel	Ball	Center	10
	Ball	Center	30
	Ball	Center	35
	Ball	Center	55
	Ball	Center	60
	Ball	Center	65
	Ball	Center	70
	Ball	On stiffener	10
	Ball	On stiffener	30
	Ball	On stiffener	35
	Ball	On stiffener	55
	Ball	On stiffener	60
	Ball	On stiffener	65
	Ball	On stiffener	70

III. Numerical Results and Discussion

A. Buckling Loads of Virgin Panels

Linear eigenvalue analyses were performed for all virgin panels before impact to compute their initial buckling loads. Two opposite edges of the panels were simply supported and the other two edges were free. The buckling load was applied to the simply supported edges. The first five buckling modes and their associated buckling loads were calculated. However, the lowest buckling load, called the critical buckling load, was selected as the reference value to be compared with the compressive failure load after impact damage. The critical buckling loads for the unstiffened and stiffened virgin

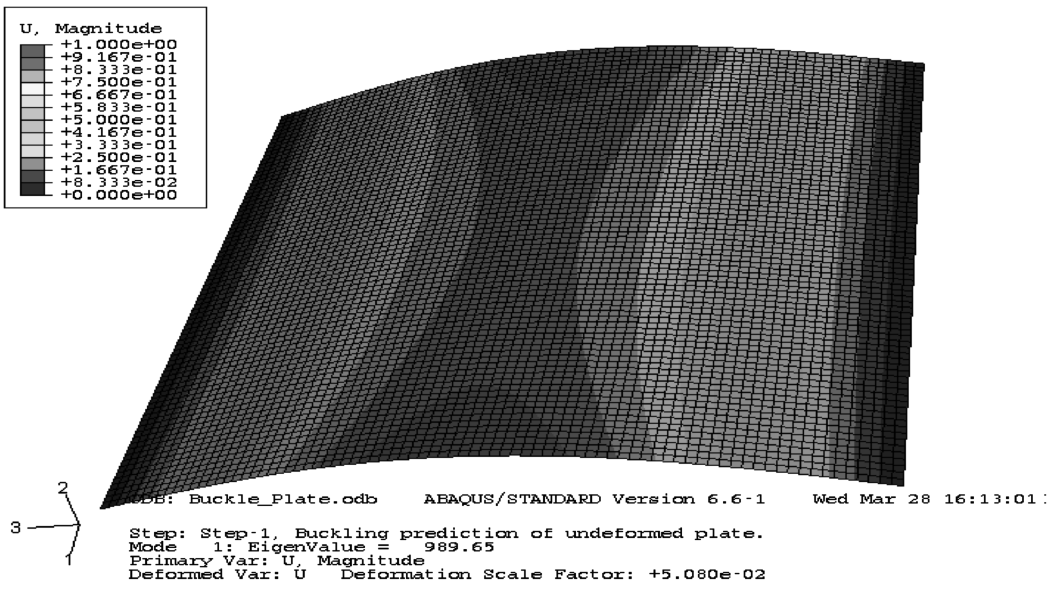

Fig. 3 First buckling mode of virgin unstiffened panel.

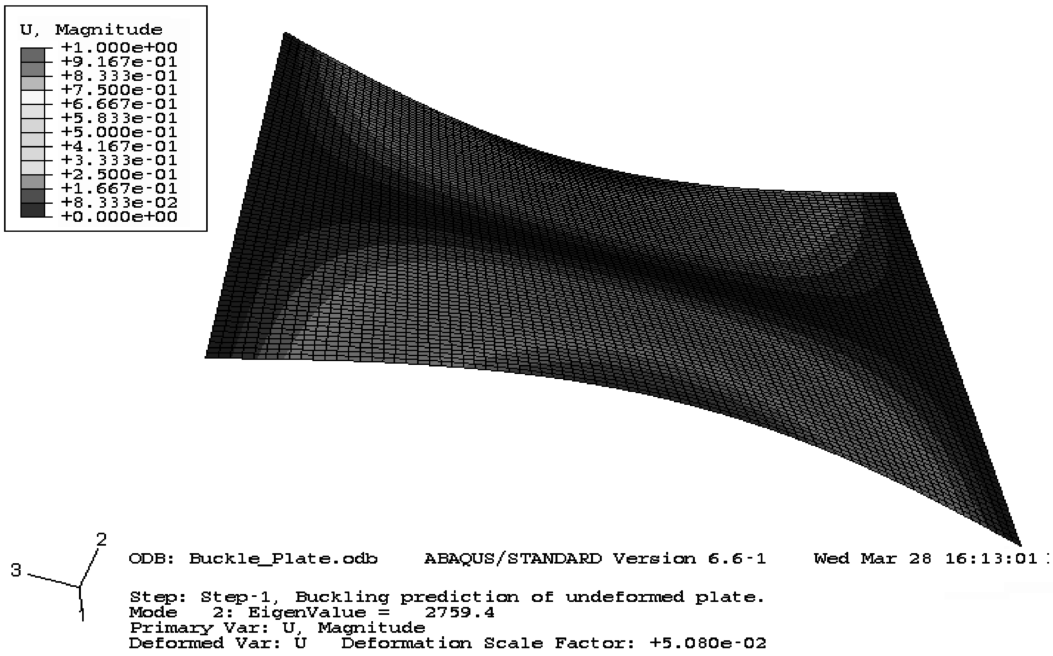

Fig. 4 Second buckling mode of virgin unstiffened panel.

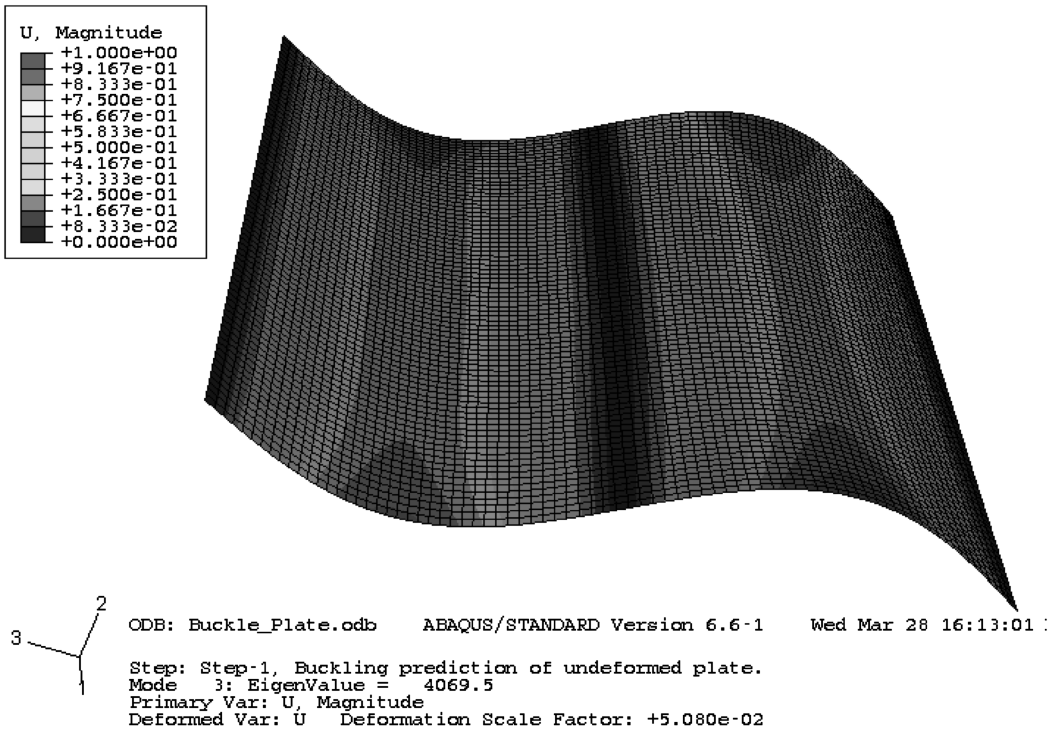

Fig. 5 Third buckling mode of virgin unstiffened panel.

panels were 990 and 15,920 N, respectively. The first four buckling mode shapes for unstiffened virgin panels are shown in Figs. 3–6.

B. Dynamic Impact Analysis

The impactor was a 0.0254-cm-radius (1-in.-radius) rigid ball. The rigid ball impacted each panel at various velocities and locations, as shown in Table 2, creating different dent sizes and depths. As expected, the dent sizes and depths generally increased with the increasing impact velocity. Dent sizes varied from 6.35 cm (2.5 in.) to slightly less than 15.24 cm (6.0 in.) in diameter. The depth of dents varied from about a 0.3175 cm ($\frac{1}{8}$ in.) to a little over 6.35 cm (2.5 in.). Although dent sizes and depths were not the same for the deformed stiffened and unstiffened panels subjected to the same impact condition, both did show the same trend of an increase in dent sizes and depths with respect to an increase in impact velocity. At lower impact velocities, however, it was difficult to determine the dent radius because the dent sizes were too small to measure accurately with finite element mesh size of 0.635 cm (0.25 in). For instance, for the stiffened panel impacted at the velocity of 10 m/s at the center, the dent size was probably less than 0.635 cm and therefore too small to be measured. The existence of a dent was confirmed by the contour plot of equivalent plastic strain.

Figure 7 shows the plot of the normalized dent diameter with respect to the panel thickness versus impact speed. The plot showed that initially there was an increase in the dent size with an increasing

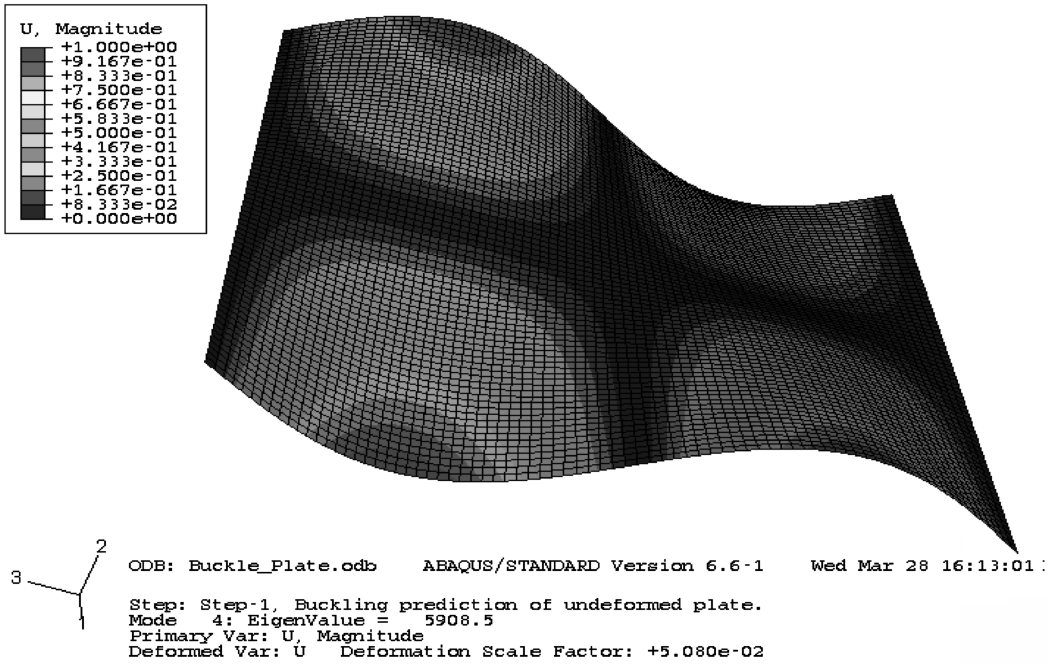

Fig. 6 Fourth buckling mode of virgin unstiffened panel.

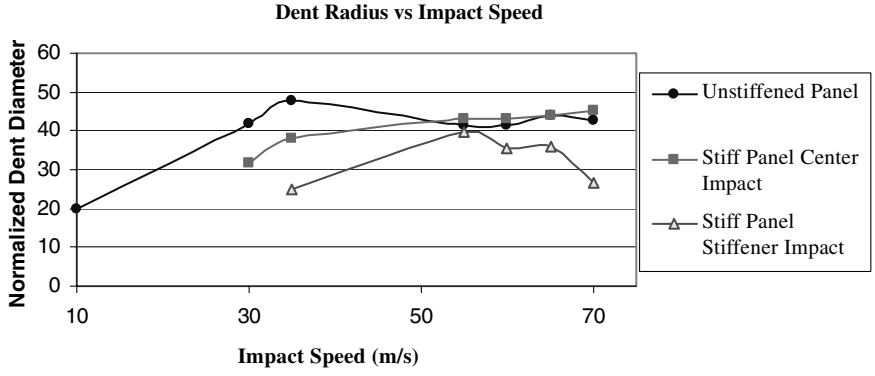

Fig. 7 Plot of dent diameter vs impact speed.

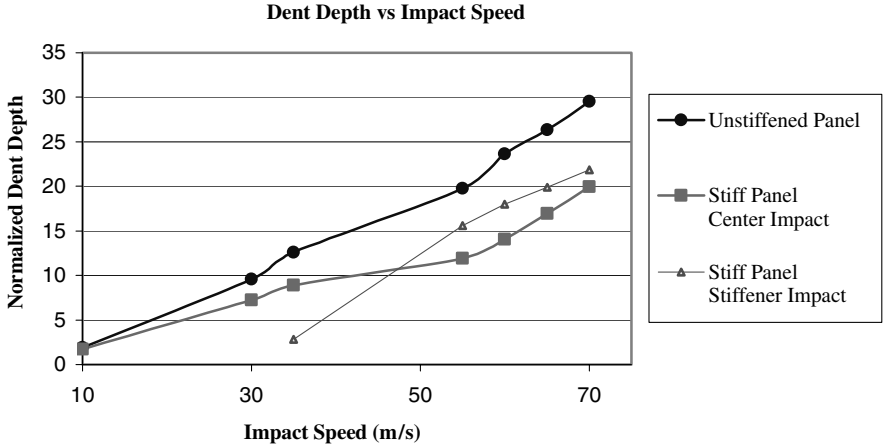

Fig. 8 Plot of dent depth vs impact speed.

impact velocity for all three cases. For the center impact of stiffened and unstiffened panels, the dent sizes showed a large increase from a low velocity (10 m/s) to a higher velocity (30 m/s) and slowed down or stabilized at a much higher velocity. The dent size of the stiffened panel with an impact at 10 m/s was too small to measure even from the contour plot of equivalent plastic strain.

For the direct stiffener site impact, however, the figure showed that the dent radius experienced a large jump initially and decreased at

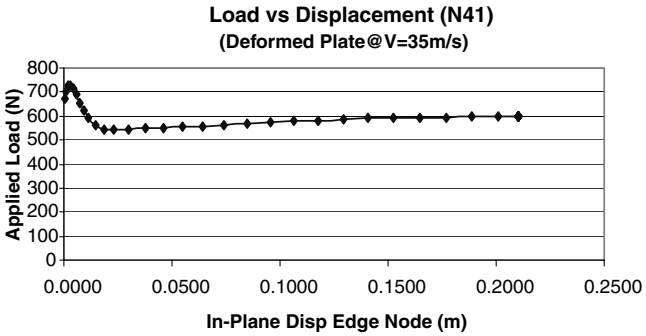

Fig. 9 In-plane compressive load-displacement curve for unstiffened panel after impact at $V = 35$ m/s.

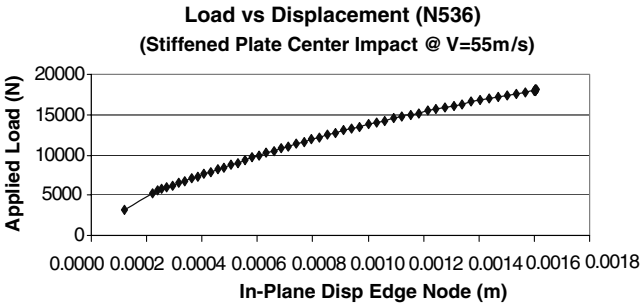

Fig. 11 In-plane compressive load-displacement plot for deformed stiffened plate after impact at 55 m/s.

high velocities. There is no clear explanation for the decrease at this time. This phenomenon needs to be further investigated.

The dent depths were determined by the maximum transverse displacement shown on the displacement contour plot of each deformed panel. Figure 8 shows that the normalized dent depth with respect to the panel thickness increases monotonically as a function of the impact speed. Both the unstiffened panel and the stiffener site impact panel showed a nearly linear relationship between the dent depth and the impact speed. However, the stiffened panel with the center impact indicated a less linear relationship.

C. Postbuckling Compressive Failure Analysis

Following the dynamic impact analyses, the deformed panels (including the residual stresses and strains) were imported into the next models and were subjected to in-plane compressive loading. The compressive failure loads from the postbuckling compression analyses were determined from the load and displacement data. For example, for the unstiffened panel, critical failure loads could be read directly from their load-vs-displacement curves. Figure 9 shows the load-vs-displacement curve for the deformed unstiffened plate after the 35-m/s impact. The curve clearly shows the failure load at 750 N. The failure modes for unstiffened panels after various impact speeds were as expected (see Fig. 10). Their shapes were almost a half-sine curve. Similarly, the failure loads for stiffened panels were determined from the load-displacement curve. However, for the latter case, the finite element solution diverges after reaching the failure load, as shown in Fig. 11. The typical compressive failure mode is seen in Fig. 12.

The compressive failure analysis for the damaged unstiffened panel showed that certain fuselage dents seemed to increase the failure load of the panel compared with the buckling load of the virgin panel. An experimental study by Guijt [9] also noted a strengthening effect caused by existence of dents. As plotted in Fig. 13, in which the compressive failure loads were normalized with respect to the buckling load of the respective virgin panel, it can be seen that at low impact velocities, the compressive failure loads were smaller than the virgin buckling load. In fact, at the impact speed of 10, 30, and 35 m/s, the compressive failure loads were 606, 659, and 725 N, respectively, which were less than that of the virgin panel (990 N). As the impact velocity increased, the failure load continued to increase, exceeding the buckling load of the virgin panel. The failure load increased to a maximum at 1368 N and began to decrease. The increase of the failure load after a high-velocity impact is considered to be caused by the increase of bending stiffness of the protruded dent. Some analysis for this phenomenon is provided later in this section.

For the dented stiffened panel at the center, the results from the postbuckling compression analyses revealed similar behaviors as earlier. The failure load for the damaged stiffened panel started out at a slightly lower value than the virgin buckling load (15,920 N) and increased, surpassing the buckling load, to a maximum and began to decrease back down. As shown in Fig. 14, for the stiffened panel with center impact at 10 m/s, the failure load was 15,190 N. This was slightly lower than the buckling load for the virgin panel. The failure load reached a maximum value of 42,260 N at 30 m/s and started to decrease rapidly to 15,967 N at 70 m/s. These results, again, appeared to suggest a stiffening effect caused by high-velocity impacts.

For the stiffened panel with direct damage to the stiffener site, it was found that the maximum failure load was 39,230 N at the impact velocity of 55 m/s. At low impact velocities, the buckling loads were approximately 25% lower than those of the virgin panel without dent. It appeared that damage to the stiffener support at a low-velocity impact could be quite detrimental to the structure of a fuselage. The

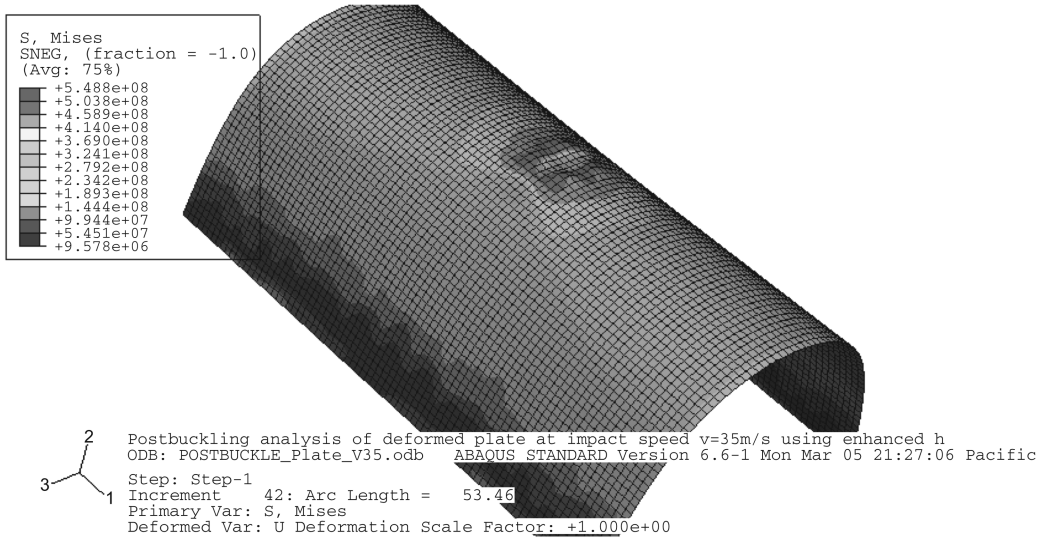

Fig. 10 Failure mode of unstiffened panel under in-plane compression after impact.

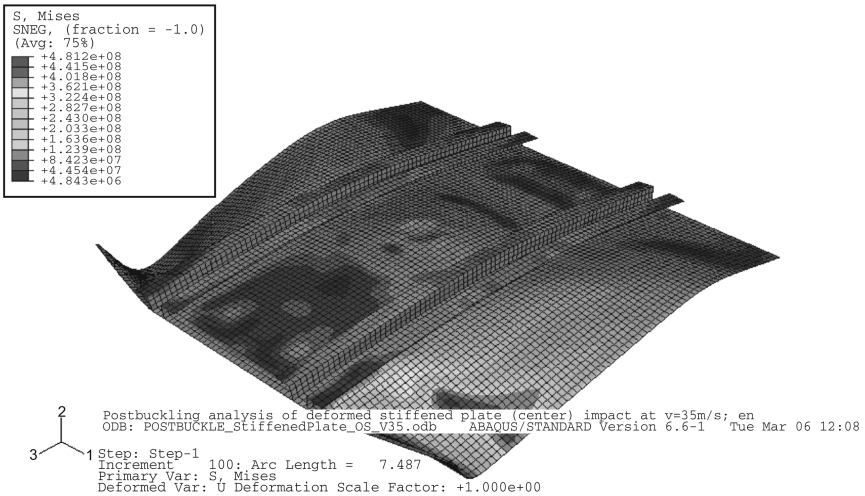

Fig. 12 Failure mode of stiffened panel under in-plane compressive load after impact at 55 m/s.

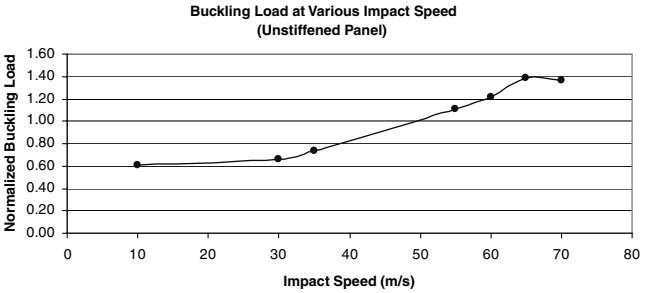

Fig. 13 Failure load vs Impact speed for dented unstiffened panel.

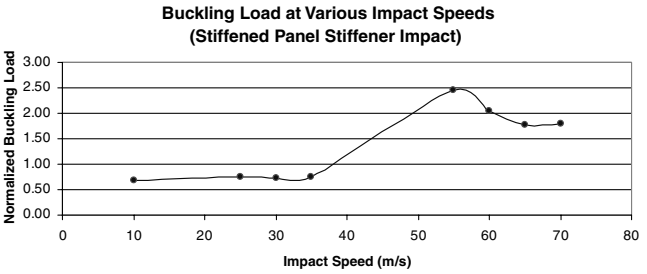

Fig. 15 Failure load vs Impact speed for dented stiffened panel with stiffener site impact.

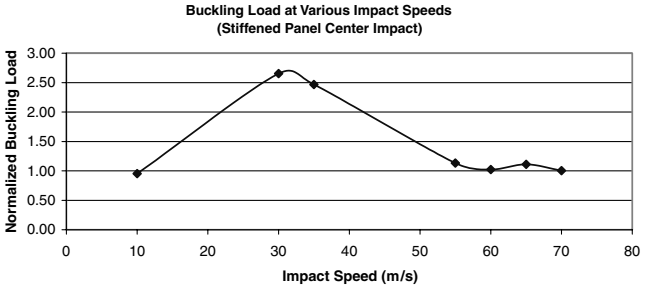

Fig. 14 Failure load vs Impact speed for dented stiffened panel with central impact.

failure-load-vs-impact-speed plot in Fig. 15 shows a summary of buckling behavior of the deformed stiffened panel at a stiffener site.

D. Linear Eigenvalue Analysis After Impact Analysis

Linear eigenvalue analyses were performed for each damaged panel after impact analysis to compute their buckling loads. The geometric shapes of the damaged panels were imported from the impact analysis models for the eigenvalue analysis. Because the linear eigenvalue analysis does not require residual stress/strain, this information was not imported. The buckling loads of the damaged panels were compared with the compressive failure loads after the impact damage. Even though the boundary conditions and the loading direction were the same for the two analyses (i.e., nonlinear postbuckling compressive failure analysis and linear eigenvalue analysis), the comparison showed, in general, a large difference in the failure loads and mode shapes between the two analyses, as seen in Table 3. For instance, at 70-m/s impact on a stiffener, the damaged stiffened panel showed a buckling load of 15,600 N, whereas the failure load from compressive failure analysis gave slightly over 28,700 N. Moreover, when comparing failure mode shapes for the same damaged panel, the postbuckling compressive analysis showed a larger deformation along the stiffener support (Fig. 16). On the other hand, the linear eigenvalue analysis showed a larger deformation on one of the free edges (Fig. 17). The next four eigenvalue mode shapes for the same panel were also very different from the postbuckling compressive failure mode. This study suggested that modeling a dent shape only without considering

Table 3 Comparison of failure loads computed from postbuckling compression analysis and linear buckling analysis after the same impact condition

Panel type	Impact location	Impact speed, m/s	Failure load from buckling analysis, N	Failure load from compression analysis, N
Unstiffened panel	Center	10	2125	606
	Center	65	7513	1368
Stiffened panel	Center	10	8978	15,186
	Center	25	20,094	13,770
	Center	55	20,687	18,044
	Center	60	23,357	16,278
	Center	65	18,858	17,690
	Center	70	6245	15,967
	On stiffener	70	15,611	28,719

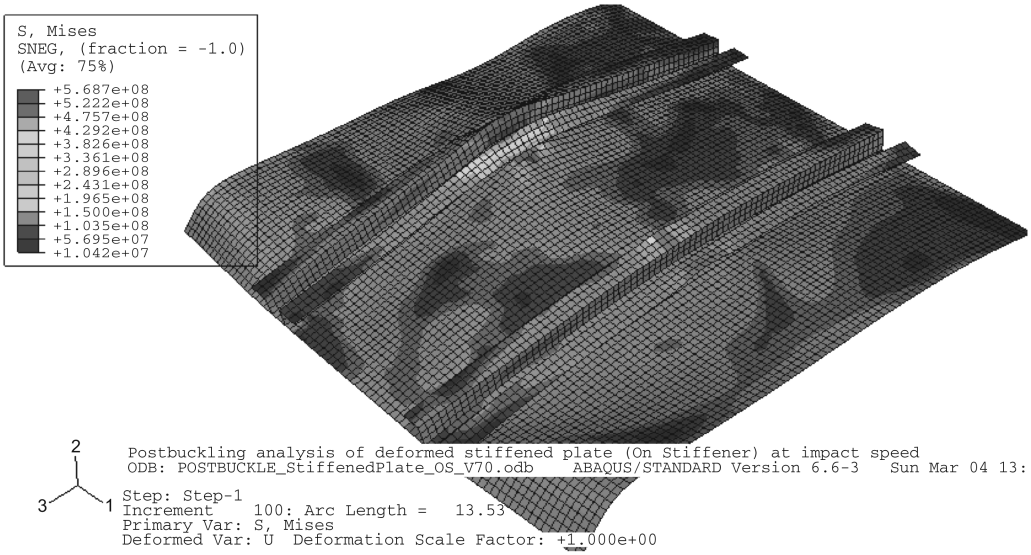

Fig. 16 Failure mode of stiffened panel with stiffener site impact at 70 m/s obtained from postbuckling compression analysis.

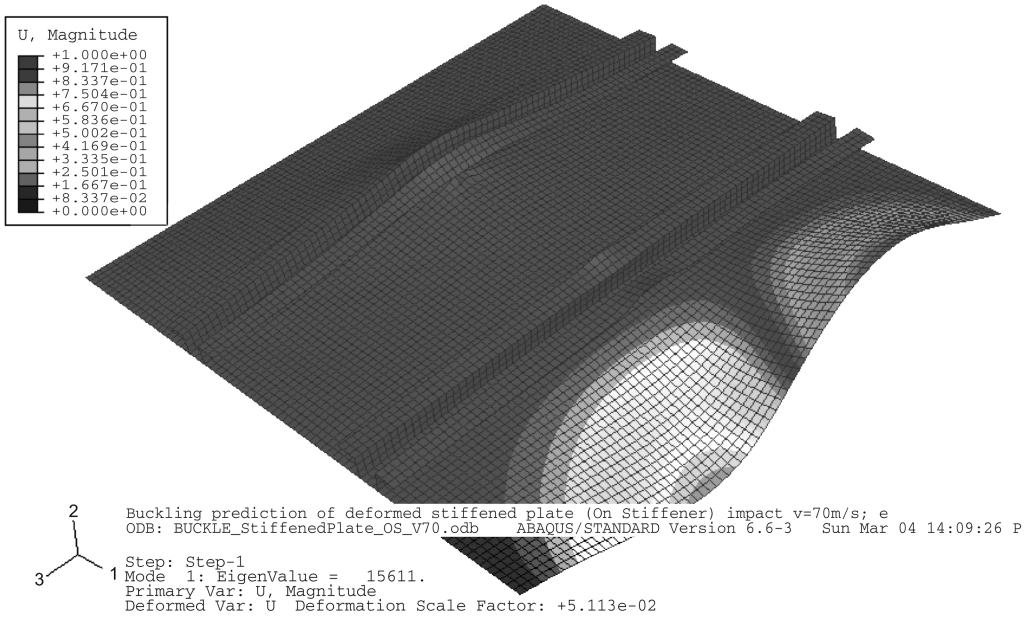

Fig. 17 Failure mode of stiffened panel with stiffener site impact at 70 m/s obtained from linear eigenvalue analysis.

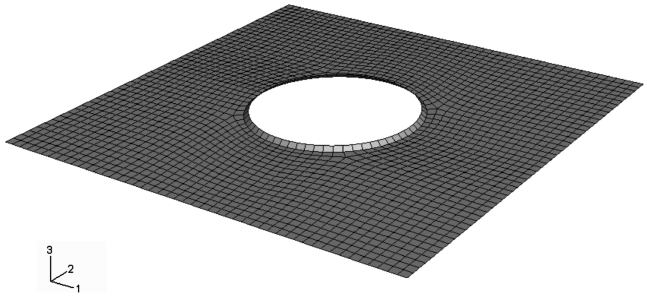

Fig. 18 Finite element mesh of a flat panel with protruding edge around central cutout.

residual stresses and strains would not produce an accurate failure load. In other words, it is important to know the residual stresses and strains associated with a dent for a reliable prediction of the failure load.

E. Study of Stiffening Effect Associated with Dents

From the compressive failure analysis, it was noticed that an existence of a dent seemed to cause a strengthening of the deformed fuselage panels, as discussed. The present study showed that at a lower impact velocity, the failure load was smaller than that of the undamaged virgin panel. At a higher velocity, the failure load rose above that of the virgin panel and reached a maximum at a critical impact velocity. At an impact velocity greater than the critical velocity, the buckling load began to decrease. This important observation was made in both unstiffened and stiffened panels.

By examining the dent sizes and depths, the dent shape was not significant at a low impact velocity. The dent was a very small localized deformation at the impact site compared with the rest of the panel. However, the local residual stress at the dent caused by the impact reduced the overall strength of the panel. As a result, a very small local dent yielded the compressive failure load lower than the buckling load of the virgin plate without a dent. As the impact velocity increased, the dent shape became more significant. Then there were two competing factors. First, the dented site has a lower local strength with high residual stresses, which would reduce the

Table 4 Buckling loads for panel with cutout and edge protrusion

Protrusion height, cm	Protrusion angle	Buckling load, N
No cutout	No cutout	990
0	0	660
0.1	8.6	724
0.1	4.3	777
0.2	16.8	800
0.3	24.4	874
0.635	90	967
1.0	60.9	1047
1.0	40.8	1078
1.0	24.8	1145
2.0	59.9	3272

compressive failure load. Second, the shape of the dent played a local stiffening effect in terms of bending stiffness, which would increase the compressive failure strength. A reduction in the compressive failure load can be viewed as a negative effect, whereas an increase in the compressive failure load can be viewed as a positive effect. Thus, the net effect (i.e., negative effect subtracted from the positive effective) was negative for a low impact speed and started to increase until it became a positive value. As a result, the compressive failure load of a dented panel increased with the impact velocity. The compressive failure load eventually exceeded that of the virgin panel. After reaching a peak compressive failure load, the net effect would start to decrease, resulting in decrease of the compressive failure load.

In an attempt to support this argument, a series of finite element models were created for a panel with protrusion, as described next. The models consisted of 0.508×0.508 m flat panels with a 20.32-cm-diam (8-in.-diam) cutout at their centers. The cutout edge has a truncated conelike protrusion, as shown in Fig. 18. The protrusion size and shape were varied. In other words, the protrusion angle measured relative to the flat panel was varied along with its height. In those models, the cutout represented a reduction of strength associated with residual stresses due to impact, whereas the protrusion represented a dent.

Linear eigenvalue analyses were conducted to the panels with cutouts and edge protrusions to determine their buckling loads. These results would show the effect of the cutout and the edge protrusion on the buckling load. The latter would increase the load, whereas the former would decrease it. Table 4 summarized the results. As seen in the table, when the effect of the cutout is greater than the protrusion effect, the buckling load is lower than that of the panel without a cutout. However, as the protrusion effect (i.e., increase of bending stiffness associated the dent) becomes more dominant, the buckling load becomes much greater than that of the plate without a cutout.

IV. Conclusions

This study investigated the effect of fuselage dents on compressive failure loads using the finite element method. By modeling different impact velocities and locations, various dent shapes (sizes and depths) were created for both unstiffened and stiffened panels. An additional study was also performed to attempt to further explain the stiffening effect of fuselage dents on the compressive failure load. From this study, a few conclusions and generalizations were made based on examination of the results.

1) Depending on the dent status in a panel caused by an impact, the dent may decrease or increase the compressive failure load of the panel compared with the virgin panel without impact. This result makes it difficult to recommend a repair guideline presently. More extensive research is necessary.

2) It was observed that at a low impact velocity, failure loads of damaged panels were generally smaller than those of the virgin panels. However, as the impact velocity was increased, the failure loads also increased and eventually surpassed the buckling loads of the virgin panels. At certain critical impact velocities, the failure loads reached maximum values, after which they began to decrease. In general, the existence of a dent could strengthen a deformed panel in a certain dent size range or impact velocity.

3) A direct impact to a stiffener site at a low impact velocity was detrimental because the failure load was shown to be much less than that of the virgin panel without impact.

4) The linear eigenvalue analysis of a damaged panel did not predict the compressive failure load properly because residual stresses were not accounted in the eigenvalue analysis.

A future study will consider different shapes of impactors, multiple impacts, and initially curved stiffened panels to further understand the effect of dents on the compressive strength. In addition, their effects on shear strength will be also studied.

References

[1] Wanhill, R. J. H., "Aircraft Corrosion and Fatigue Damage Assessment," National Aerospace Lab., Rept. TP94401 L, Amsterdam, 1994.

[2] Siegel, M., and Gunatilake, P., "Remote Inspection Technologies for Aircraft Skin Inspection," *IEEE Workshop on Emergent Technologies and Virtual System for Instrumentation and Measurement*, Inst. of Electrical and Electronics Engineers, Piscataway, NJ, 15–17 May 1997.

[3] Schijve, J., "Multiple-site Damage in Aircraft Fuselage Structures," *Fatigue and Fracture of Engineering Materials and Structures*, Vol. 18, No. 3, Mar. 1995, pp. 329–344. doi:10.1111/j.1460-2695.1995.tb00879.x

[4] Barter, S., Molent, L., Goldsmith, N. and Jones, R., "An Experimental Evaluation of Fatigue Crack Growth," *Engineering Failure Analysis*, Vol. 12, No. 1, February 2005, pp. 99–128. doi:10.1016/j.engfailanal.2004.04.002

[5] Wang, L., Chow, W. T., Kawai, H., and Atluri, S. N., "Residual Strength of Aging Aircraft with Multiple Site Damage/Multiple Element Damage," *AIAA Journal*, Vol. 36, No. 5, May 1998, pp. 840–847.

[6] Diamantakos, I. D., Labeas, G. N., Pantelakis, S. G., and Kermanidis, T. B., "A Model to Assess the Fatigue Behaviour of Ageing Aircraft Fuselage," *Fatigue and Fracture of Engineering Materials and Structures*, Vol. 24, No. 10, 2001, pp. 677–686. doi:10.1046/j.1460-2695.2001.00423.x

[7] Rankin, C. C., Brogan, F. A., and Riks, E., "Some Computational Tools for the Analysis of Through Cracks in Stiffened Fuselage Shells," *Computational Mechanics*, Vol. 13, No. 3, 1993, pp. 143–156. doi:10.1007/BF00370132

[8] Goranson, U. G., "Fatigue Issues in Aircraft Maintenance and Repairs," *International Journal of Fatigue*, Vol. 20, No. 6, July 1998, pp. 413–431. doi:10.1016/S0142-1123(97)00029-7

[9] Guijt, C., "New Structural Guidelines for Dent Allowables on Fuselages," 2005 USAF Structural Integrity Program (ASIP) Conference, 2005

[10] ABAQUS/CAE User's Manual, Ver. 6.6, Hibbit, Karlsson and Sorensen, Providence, RI, 2006.